

PROGRESS TOWARDS MODELING THE EFFECTS OF ICE ACCRETION ON ROTORCRAFT PERFORMANCE IN HOVER AND FORWARD FLIGHT

Jeremy Bain and Lakshmi N. Sankar, Georgia Institute of Technology, Atlanta, GA, USA
T. Alan Egolf and Robert J. Flemming, Sikorsky Aircraft Corporation, Stratford, CT, USA
Richard Eric Kreeger, NASA Glenn Research Center, Cleveland, OH, USA

Abstract

A framework has been developed for computationally modelling the effects of ice accretion on a helicopter rotor. In this approach, the ice accretion models, the flow solver, the grid generator, and the aeroelastic analyses exchange data using open I/O standards. In two-dimensional compressible flow, a one-way coupling between the ice accretion modelling (LEWICE3D) and the flow analysis (OVERFLOW) in predicted the ice shape with reduced ice thickness. The double horn ice shape is correctly predicated as the angle-of-attack and liquid water content increases. Subsequent 3-D simulations have also been performed where LEWICE3D is coupled to TURNS, a flow analysis for modelling rotors in hover. Results are presented for the UH-60A Blackhawk Rotor to assess the effects of ice growth on the rotor power at constant thrust.

1. INTRODUCTION

The cost and time to certify or qualify a rotorcraft for flight in forecast icing has been a major impediment to the development of ice protection systems for helicopter rotors. Development and flight test programs for aircraft that have achieved certification or qualification for flight in icing conditions have taken many years, and the costs have been very high. NASA, Sikorsky, and others have conducted research into alternatives to natural in-flight icing tests to provide information for the development of ice protection systems and to substantiate the airworthiness of a rotor ice protection system (Ref. 1-11). Much progress has been made both in ice accretion modeling and in coupling the ice accretion models to rotary wing aerodynamic analyses^{12,13}. Many of these approaches however were developed for 2D airfoil sections and 3D wings with ice formation modeled in a strip theory fashion.

Ice growth is separated into dry and wet growth. In general, wet growth is more challenging due to the requirement to account for the melting, freezing, and runback of water. The ice growths shown in Figure 1, especially the double horned shape, can result in significant increases in power required on the order of 20%.

2. METHODOLOGY

Given the complex, tightly coupled, multi-physics problem that is being solved, a modular approach is necessary. Although the present work employs specific versions of Computational Fluid Dynamics (CFD), Computational Structural Dynamics (CSD), and ice accretion tools, it is not limited to only these tools. The framework employs open interfaces for

coupling the analyses, permitting replacement of current generation tools with next generation analyses.

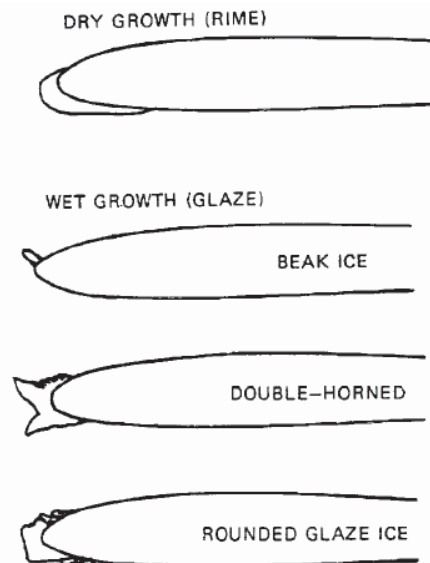


Figure 1. Ice Shape Types⁹

The framework is shown in Figure 2. First, a forward flight trim solution is obtained for the clean rotor. In forward flight, this is obtained using CFD/CSD coupling¹⁴. This methodology has been widely used with a variety of CFD and CSD solvers^{15, 16}. A rotor revolution is typically on the order of 1/4 a second and a typical full scale icing test case is on the order of 15 minutes. Due to the computational cost of running CFD/CSD coupling, it is not practical to perform simultaneous integration in time of the CFD/CSD/icing analyses for 3600 revolutions. The ice accretion is a slow process. The flow field does

not change from revolution to revolution appreciably and may be sampled (or computed) only at selected instances in time. Discrete events such as shedding would produce an abrupt variation in the flow field over the rotor, and will require a recalculation of the flow field and retrim when a shedding event is detected.

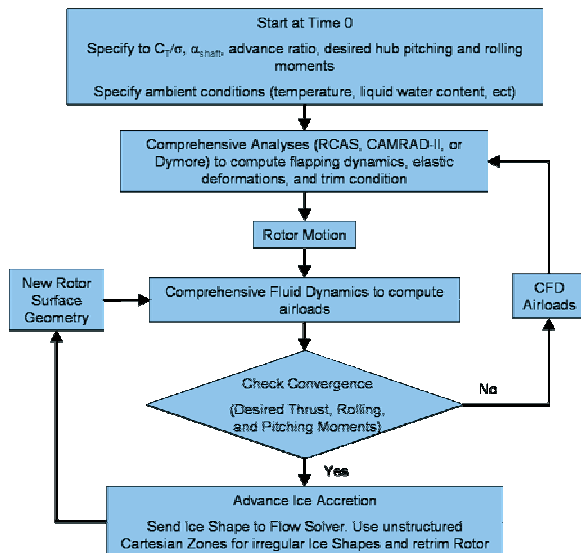


Figure 2. Framework for Coupling Ice Accretion and Aeromechanics Analyses

The computed flow field is passed to LEWICE3D which computes the ice accretion over several minutes of ice build-up for representative sections on the rotor blade. The user may select the number of radial locations where the ice shape is computed. Previous experimental experience has shown that the torque rise due to ice accretion is nonlinear with time and typically levels off after a set period of time⁹. Once the ice shapes are obtained along the rotor span, a new grid is generated. Irregular ice shapes represent a challenge for structured grids and an unstructured or unstructured Cartesian solver may need to be used. At this writing, the present authors have only used structured grids for these initial studies.

Using the new grid, a new CFD/CSD coupled analysis is done to retrim the rotor for the desired flight conditions. Currently in hover this is being done once to represent one relatively large ice growth interval. In the future for forward flight, this process will be repeated several times allowing the ice to grow over time intervals representing an icing flight condition of long duration. This will provide a quasi-steady prediction of the effect of ice growth on power, vibration, and airloads over the duration of the flight.

The various interfaces between the codes are being automated and made generic so that little user

intervention is needed during the analysis. The modularity also allows the individual code modules to be updated independent of the remaining framework. Validation of the methodology and identification of areas that require future work is being done using NASA and Sikorsky test data for airfoils, wings, model rotors, and full-scale rotors.

2.1. LEWICE3D Ice Accretion Software

LEWICE3D is a grid-based ice accretion software analysis tool that can interface with a variety of 3-D computational solvers for computing ice shapes on three-dimensional external surfaces^{12,13}. The streamlines and ice particle trajectories are computed using the provided flow solution. The ice accretion analysis is divided into 2-D sections-of-interest. A 2D heat transfer module is used to calculate the ice growth along the streamline. LEWICE3D and previous versions have been extensively validated for a wide range of airfoils and icing conditions.

2.2. OVERFLOW

The Navier-Stokes computational fluid dynamics code OVERFLOW Version 2.1y was used for the 2-D airfoil simulations. OVERFLOW, developed by NASA, uses overset structured grids for a wide variety of problems including rotorcraft aerodynamic simulations^{17,18}.

2.3. TURNS

TURNS (Transonic Unsteady Rotor Navier Stokes) was developed to analyze rotors in hover¹⁹. TURNS solves the 3-D compressible Navier-Stokes equations in integral form using a sixth order symmetric total variation diminishing scheme²⁰.

2.4. Interface

LEWICE3D uses flow field information from standard FORTRAN unformatted, double precision, multigrid PLOT3D grid and solution files. Scripts were written to change the output of OVERFLOW and TURNS into this format. The solution reference frame was also changed from a moving blade to a fixed blade reference frame for LEWICE3D. The ice shapes from LEWICE3D were combined with the original airfoil shape. These modified airfoils were then transformed so that they are at zero degrees angle-of-attack of the original airfoil and have a chord of unity for the TURNS grid generator.

3. RESULTS

3.1. Two-Dimensional Validation

A large body of icing validation using LEWICE3D exists but is primarily focused on the low Mach

number regime. Helicopters have hover tip Mach numbers around 0.7 and the advancing blade tip Mach number can exceed 0.85 in high speed flight. To assess the ability of the OVERFLOW and LEWICE3D coupled analysis to model ice accretion, calculations were done for the SC1094R8 airfoil at two experiment conditions⁹.

A C-grid of dimensions 377x85 was created with a y^+ of 0.5 for better prediction of heat transfer. The first test is at zero degrees angle-of-attack with the properties in Table 1. The low liquid water content forms a rounded glaze ice shape. The computed ice shape and experiment ice shape are compared in Figure 3. The ice shapes are qualitatively similar but the computed ice shape thickness is under-predicted. The ice thickness is sensitive to the prediction of heat transfer from the flow solution. A recent bug fix in the LEWICE may improve predictions but was not evaluated. When used in conjunction with a viscous flow analysis, it is customary to pass on the nominal value of the computed boundary layer thickness to LEWICE3D. It was found that the ice shape can be sensitive if too large of a boundary layer thickness is used. In the present study, a nominal boundary layer thickness of $5e-4$ chords was used.

Table 1. SC1094R8 Test Case 1

Angle-of-Attack	0°
Chord	0.1524m
Mach Number	0.57
Ambient Temperature	-10°C
Liquid Water Content	0.58 g/m ³
Ice Accretion Duration	45s
Droplet Size	20µm

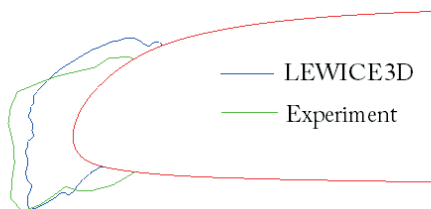


Figure 3. Zero Degree SC1094R8 Test Case

New grids for the ice shapes from the test data and LEWICE3D were generated and then analyzed in OVERFLOW to examine the effects of ice accretion on airloads. The flow field was compared to that of the clean airfoil. Table 2 shows the change in airloads. It appears that this one-way coupling approach adequately captures the changes to the airloads. The pressure distributions for the clean and iced airfoil configurations are shown in Figure 4. The ice shape tripled the drag by producing a larger stagnation zone on the leading edge due to the rounded glaze ice shape, followed by total pressure losses downstream. The nose down pitching moment is nearly doubled, both in the experiment ice

shape and the computed ice shape, compared to the baseline clean shape.

Table 2. Ice Shape Effects at 0 degrees

	Cl	Cd	Cm	ΔCl	ΔCd	ΔCm
Clean Airfoil	0.206	0.010	-0.0235	-	-	-
Experiment Ice Shape	0.202	0.033	-0.0429	-0.004	0.023	-0.019
LEWICE3D Ice Shape	0.198	0.038	-0.0389	-0.008	0.028	-0.015

A second test case was run at six degrees angle-of-attack and a higher liquid water content and is summarized in Table 3. This condition is transonic due to the combination of moderate Mach number and angle-of-attack. While not common in a hovering helicopter rotor, transonic flow is a dominating feature on the advancing blade in forward flight for most helicopter rotors. This condition forms a double horn shown in Figure 5. The computed ice thickness is underpredicted and there is more growth on the upper surface than observed in the experiment. LEWICE3D uses an internal aerodynamics module to compute the change in the local aerodynamics during the ice accretion process. This method becomes less accurate in transonic and separated flow.

The effect of ice accretion on airloads is shown in Table 4. The double horn disrupts the suction peak on the upper surface and causes separated flow on the upper and lower surface shown in Figure 6. This dramatically reduces the lift, increases the drag, and increases the nose down pitching moment. The calculations with the LEWICE3D ice shape predicted high nose down pitching moment than those with the the measured ice shape due to the higher roughness of the LEWICE3D based ice shape. The experiment ice shape is smoothed by the ice shape tracing process in the experiment and by digitization of the ice shape for grid generation.

Table 3. SC1094R8 Test Case 2

Airfoil	SC1094R8
Chord	0.1524m
Mach Number	0.59
Ambient Temperature	-10°C
Liquid Water Content	1.12 g/m ³
Ice Accretion Duration	45s
Droplet Size	20µm

Table 4. Ice Shape Effect at 6 Degrees

	Cl	Cd	Cm	ΔCl	ΔCd	ΔCm
Clean Airfoil	0.804	0.042	-0.0022	-	-	-
Experiment Ice Shape	0.532	0.089	-0.0152	-0.272	0.048	-0.013
LEWICE3D Ice Shape	0.536	0.097	-0.0466	-0.268	0.055	-0.044

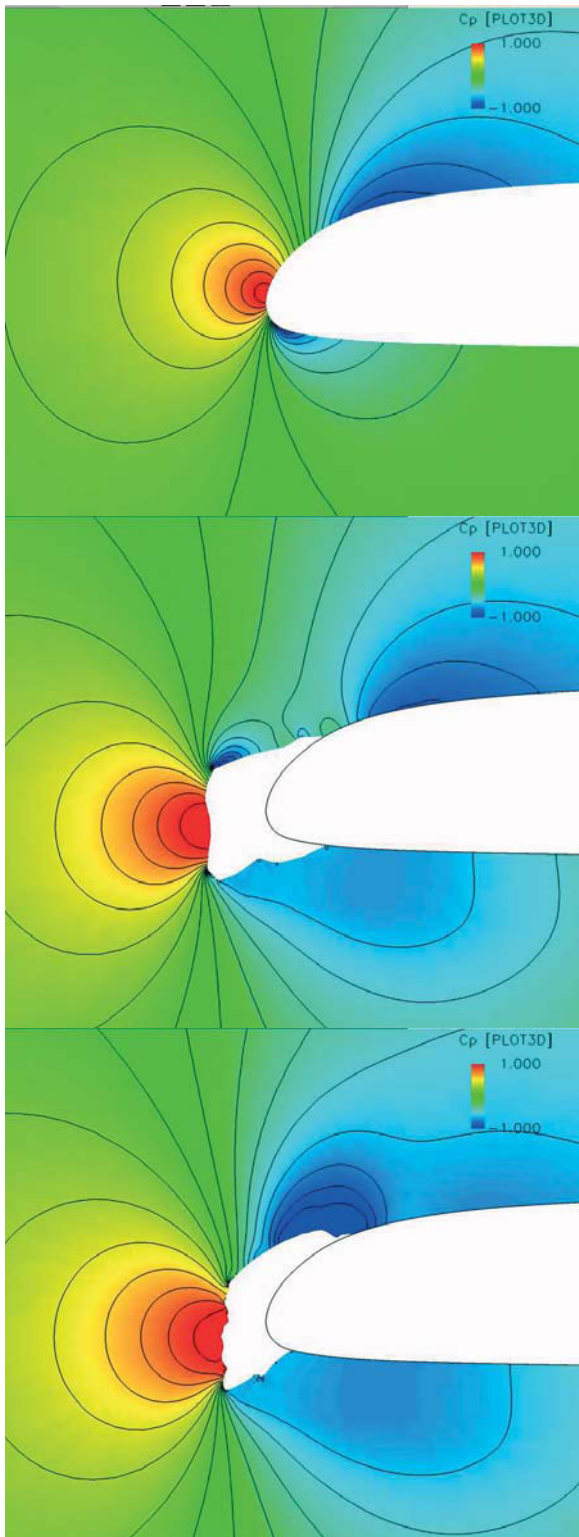


Figure 4. Case 1 Pressure Distributions with a Clean Airfoil, Experiment Ice Shape, and LEWICE3D Ice Shape

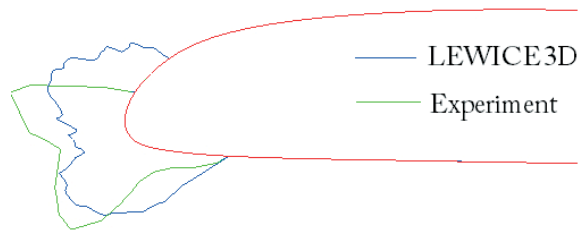


Figure 5. Six Degree SC1094R8 Test Case

3.2. Hovering Rotor Analysis

The UH-60A rotor is a four bladed articulated rotor with a nonlinear twist. It is untapered and has a 20° sweep at $r/R=0.926$. The SC1095 airfoil is the main airfoil with the SC1094R8 providing additional lift from approximately $r/R=0.5$ to 0.82 . TURNS was used to compute a hovering solution at a common mission gross weight of approximately 17000 lbs. An ice accretion analysis was done over a 15 minute period at several radial stations. The icing conditions are -10°C , 84312 Pa, ice droplet size of $20\mu\text{m}$, and liquid water content of 0.528 grams per cubic meter. These conditions are similar to the zero degree SC1094R8 case. Figure 7 shows the ice shapes at several radial stations. The ice shapes are rounded glaze ice similar to the zero degree two dimensional case but have reduced thickness due to the longer chord and the relatively smaller ice particles. Since a shedding model accounting for centrifugal force is not yet available in this simulation, no ice was allowed to accumulate outboard of $r/R=0.95$.

The TURNS grid generator was used to create the blade surface and the initial C-H-grid volume. Elements of the Chimera Grid Tools¹ were then used to increase the leading edge density in the leading edge region while preserving the original C-H-grid structure.

The iced rotor was initially run at the same collective setting as the clean rotor. The collective was then increased until the thrust was within 2% of the clean rotor. The thrust, torque, and figure of merit are compared in Table 5. The figure of merit is reduced from 0.723 to 0.622 due to the 13% rise in power required. The radial thrust and torque are shown in Figures 8 and 9. The iced rotor has significantly reduced sectional thrust compared to the clean rotor once the ice shapes increase in thickness around $r/R=0.7$. The ice shape disrupts the suction peak on the airfoil as shown in Figures 10 and 11. The increased collective required to maintain thrust requires increasing the loading on the tip of the blade. This causes the lift distribution to be less triangular and increases induced power losses.

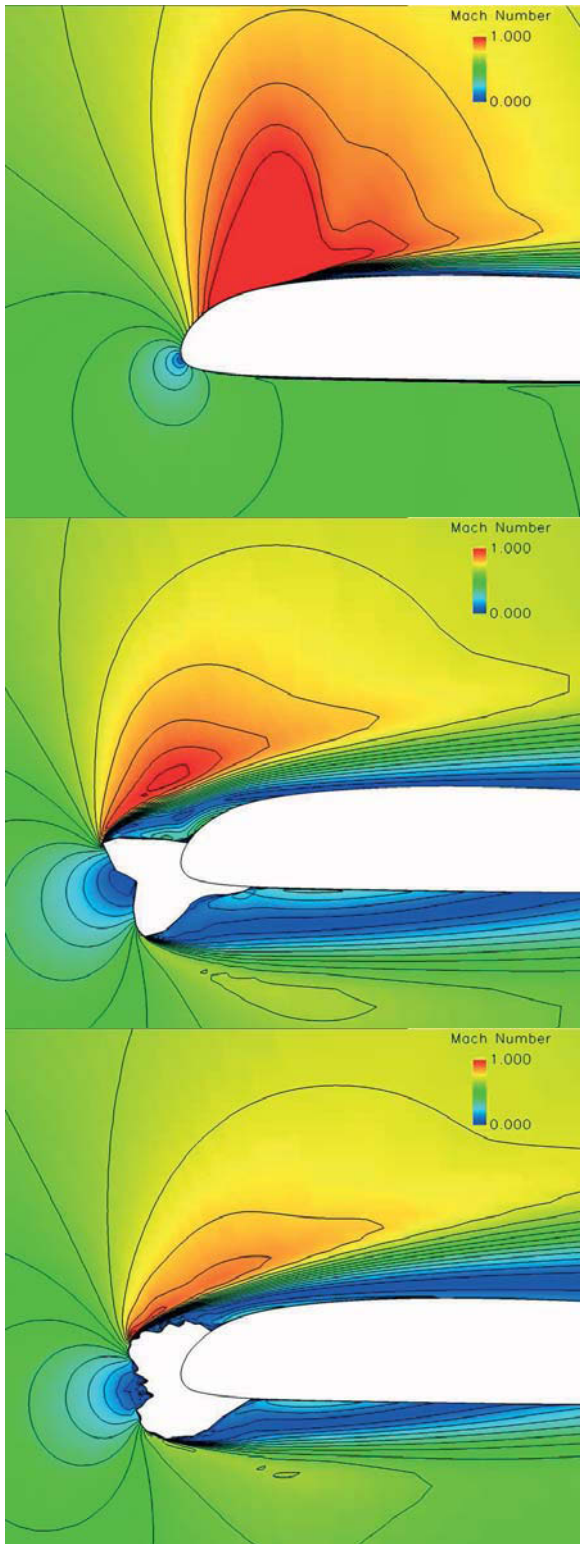


Figure 6. Case 2 Pressure Distributions with a Clean Airfoil, Experiment Ice Shape, and LEWICE3D Ice Shape

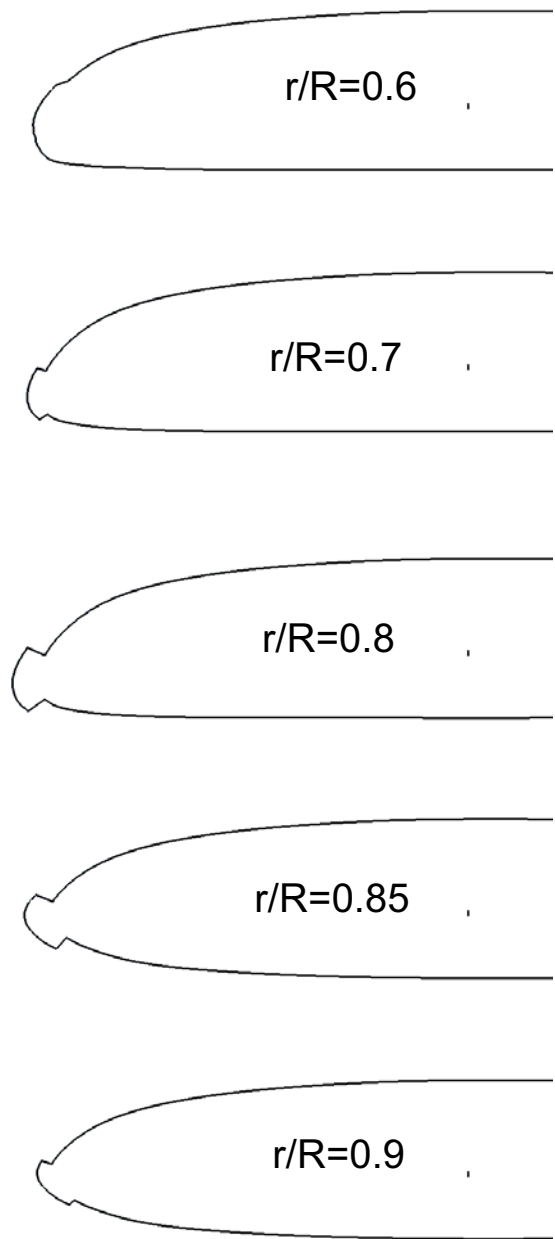


Figure 7. Ice Shapes at Several Rotor Stations

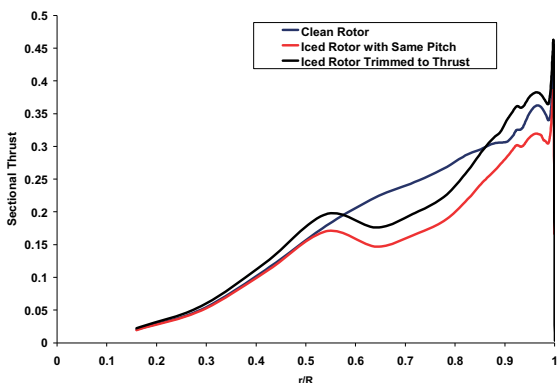


Figure 8. Sectional Thrust

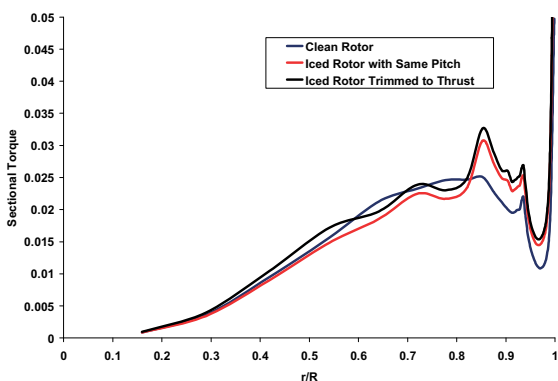


Figure 9. Sectional Torque

Table 5. Performance Results in Hover

	C_T	C_Q	FM
Clean Rotor	6.55E-03	5.19E-04	0.723
Iced Rotor with Same Pitch	5.37E-03	5.30E-04	0.526
Iced Rotor Trimmed to Thrust	6.44E-03	5.88E-04	0.622

4. CONCLUSIONS AND RECOMMENDATIONS

A framework for modelling the effects of ice accretion on the performance of rotors has been developed and preliminary results have been presented. Although only 2-D and hover calculations have been presented in this work, the framework is general enough to model rotors in forward flight. The coupled CFD approach allows aerodynamic effects (decrease in lift, increase in torque, and rotor drag) as well as structural loads to be modelled accurately. Encouraging preliminary results have been obtained and presented in a hover mode of operation.

Additional work is being done where the present one-way coupling CFD/LEWICE3D approach is replaced with a two-way coupling process where the ice accretion affects the flow field and vice versa. Work is also in progress on the assessment of grid density, time steps, turbulence model, and surface heat transfer rate calculation models on the computed ice shapes. Finally, the entire coupling

process is being automated using scripts, so that information flows seamlessly between all the modules (CFD, CSD, ice accretion model, grid generators, post-processors) with minimal user intervention. This will allow for the extension to forward flight applications.

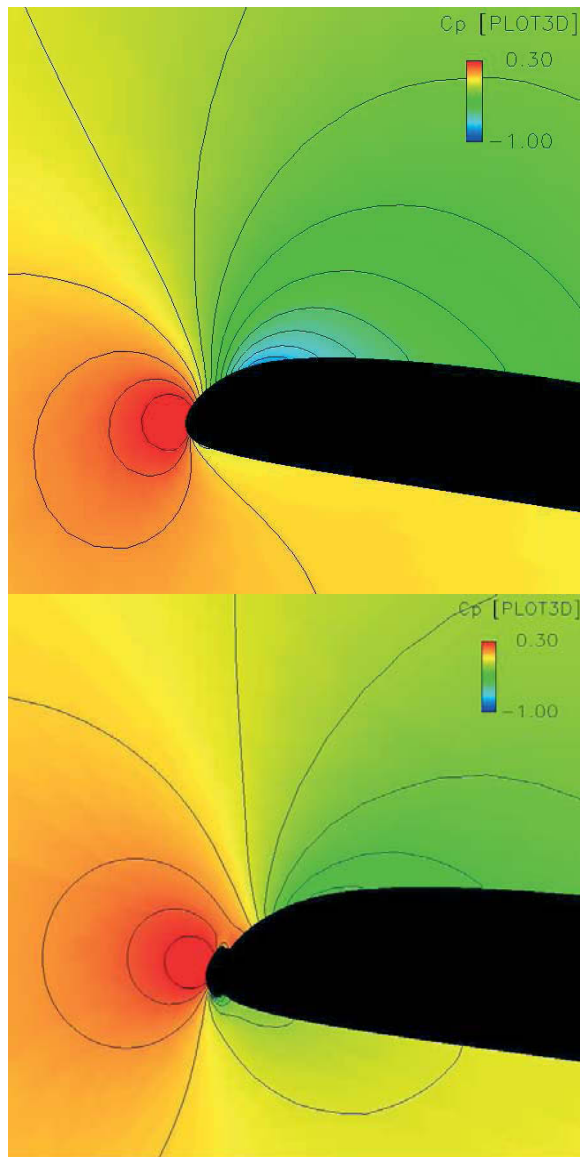


Figure 10. Pressure Distribution of Clean and Iced Rotor at $r/R = 0.72$ at Same Pitch

ACKNOWLEDGEMENTS

This work was supported under the NASA NRA Co-operative Agreement: NNX08AU71A.

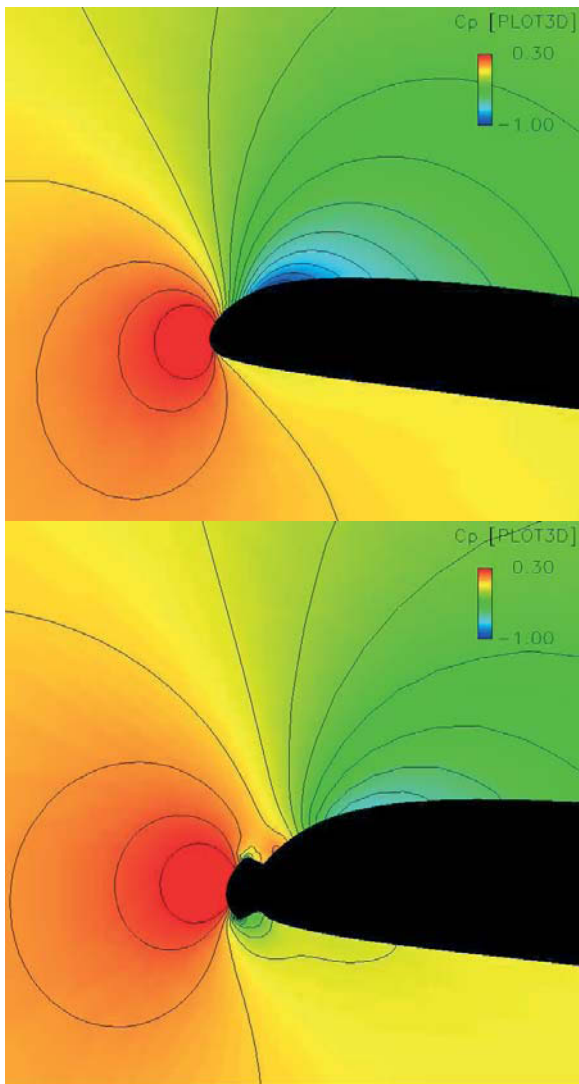


Figure 11. Pressure Distribution of Iced Rotor at Same Pitch at $r/R = 0.82$

REFERENCES

- [1] Flemming, R.J. and Britton, R., "Model Rotor Icing Tests in the NASA Icing Research Tunnel," NASA TM 104351 and AGARD 496-9, 1991.
- [2] Flemming, R.J., Bond, T, and Britton, R., "Results of a Sub-scale Model Rotor Icing Test," NASA TM 103709 and AIAA-91-0660.
- [3] Britton, R., Flemming, R.J., Bond, T, "An Overview of a Model Rotor icing Test in the NASA Lewis Icing Research Tunnel," AIAA-94-0716.
- [4] Britton, R. and Flemming, R.J., "Role of Wind Tunnels and Computer Codes in the Certification and Qualification of Rotorcraft for Flight in Forecast Icing," NASA TM 106747.
- [5] Flemming, R.J. and Saccullo, A., "Tests of a Model Main Rotor in the NASA Lewis Research Center Icing Research Tunnel," NASA CR 189071, January 1991.
- [6] Flemming, R.J., "Experimental Investigation of the Effects of Ice Accretion on a Model Rotor in the NASA Glenn Research Center Icing Research Tunnel," RITA TR 02-D-07-03.1-P3.
- [7] Flemming, R.J. and Thomas D. Parsons, "Rotor Airfoil Ice Protection Systems - Final Report for 1997-99 NRTC/RITA Icing Projects," SAC SER-510490 and BHTI 699-099-512, 2000.
- [8] Flemming, R.J., "Icing Tests of UH-60A/L Rotor Blade Erosion Coatings in the NASA Glenn Research Center Icing Research Tunnel," SAC SER-703370, 10/31/2005.
- [9] Flemming, R.J. and Lednicer, D.A., "High Speed Ice Accretion on Rotorcraft Airfoils," NASA CR-3910, 1984.
- [10] M. P. Simpson and P.M. Rendert, "Certification and operation of Helicopters in Icing Environments", AIAA-98-0075.
- [11] Tsao, Jen-Ching and Kreeger, Richard, E., "Evaluation of scaling Models for Rotorcraft Icing," AHS Annual Forum, May 2009.
- [12] Wright, W. B., "Validation Results for LEWICE 3.0" NASA/CR-2005-213561, March 2005.
- [13] Wright, W.B., Potapczuk, M., Levinson, L., "Comparision of LEWICE and GlennICE in the SLD Regime", AIAA-2008-439.
- [14] Potsdam, M., Yeo, H., Johnson, W., "Rotor Airloads Preciction using Loose Aerodynamic-Structural Coupling" AHS 60th Annual Forum, June 7-10, 2004.
- [15] Bhagwat, M.J., Dimanlig, A., Saberi, H., Meadowcroft, E., Panda, B., and Strawn, R. "CFD/CSD Coupled Trim Solution for the Dual-Rotor CH-47 Helicopter Including Fuselage Modeling," AHS Specialist Conf, Jan 2008.
- [16] Bain, J., Sankar, L. N., Prasad, J. V. R., Bauchau, O., Peters, D. A., He, C., "Computational Modeling of Variable-Droop Leading Edge in Forward Flight," Journal of Aircraft (0021-8669) 2009.
- [17] Buning, P.G., Chiu, I.T., Obayashi, S., Rizk, Y.M. and Steger, J.L., "Numerical Simulation of the Integrated Space Shuttle Vehicle in Ascent", AIAA 88-4359.
- [18] Chan, W. M. "The OVERGRID Interface for Computational Simulations on Overset Grids", 32nd AIAA Fluid Dynamics Conference, St. Louis, Missouri, June 2002. AIAA 2002-3188.
- [19] Srinivasan, G.R., Baeder, J.D., Obayashi, S., McCroskey, W.J., "Flowvield of a Lifting Rotor in Hover: a Navier-Stokes Simulation", AIAA Journal, 1992. 30(10): p. 2371-2378.
- [20] Usta, E., "Application of Symmetric Total Variation Diminishing Scheme to Aerodynamics of Rotors" PhD thesis, Georgia Institute of Technology, August 2002.